PAPER

Unconventional Hanle effect in a highly ordered CoFe/MgO/*n*-Si contact: non-monotonic bias and temperature dependence and sign inversion of the spin signal

View the article online for updates and enhancements.

You may also like

- Spin-dependent electrical hole extraction from low doped p-Si via the interface states in a Fe₃Si/p-Si structure
  A S Tarasov, A V Lukyanenko, M V Rautskii et al.

- Suppression of spin transport in ferromagnet/oxide/semiconductor junctions by magnetic impurities in the tunnel barrier
  Aurélie Spiesser, Hidekazu Saito, Shinji Yuasa et al.

- Spin transport in *p*-type germanium
  F Rortais, S Oyarzún, F Bottegoni et al.

New Journal of Physics

Unconventional Hanle effect in a highly ordered CoFe/MgO/*n*-Si contact: non-monotonic bias and temperature dependence and sign inversion of the spin signal

Kun-Rok Jeon[1]**, Byoung-Chul Min**[2]**, Il-Jae Shin**[2]**,
Chang-Yup Park**[1]**, Hun-Sung Lee**[1]**, Young-Hun Jo**[3]
and Sung-Chul Shin[1,4]

[1] Department of Physics and Center for Nanospinics of Spintronic Materials, Korea Advanced Institute of Science and Technology (KAIST), Daejeon 305-701, Korea
[2] Center for Spintronics Research, Korea Institute of Science and Technology (KIST), Seoul 136-791, Korea
[3] Nano Materials Research Team, Korea Basic Science Institute (KBSI), Daejeon 305-764, Korea
E-mail: scshin@kaist.ac.kr

Abstract. We report in this paper the unconventional bias and temperature dependence of the Hanle effect in a highly ordered CoFe/MgO/*n*-Si contact investigated by means of a three-terminal Hanle method. The spin signal and the effective spin lifetime obtained in this system show non-monotonic behavior with bias and temperature variations. Interestingly, the sign of the spin signal changes significantly with the bias voltage at a low temperature. The sign inversion is presumably ascribed to the contribution of interfacial resonant states formed at the CoFe/MgO interface or bound states in the Si surface during the spin extraction process.

[4] Author to whom any correspondence should be addressed.

IOP Institute of Physics ⬦ DEUTSCHE PHYSIKALISCHE GESELLSCHAFT

Contents

1. Introduction

The electrical injection and detection of non-equilibrium spin populations in semiconductors (SC) is crucial for spintronic applications [1–4]. Significant progress has been made on spin injection into various SC systems using spin-tunnel contacts [5–18]. Spin-tunnel contacts are a technically viable means of achieving large spin polarization in injecting carriers and effectively detecting the induced spin accumulation in SCs. Notably, the electrical spin injection and detection in a Si system was recently demonstrated using a $Co/NiFe/Al_2O_3$ tunnel contact up to room temperature; this has a significant impact on Si-based spintronics [5, 19]. However, our understanding of the spin phenomena in these systems (e.g. the magnitude and sign of the induced spin accumulation [18, 20–26], the unusual bias and temperature dependence [5, 10, 18, 19] and the unexpectedly short spin lifetime [5, 19]) remains in the initial stage. In particular, the influence of the tunnel contact on the obtained spin signal in Si is yet to be studied adequately. For example, in order to obtain high tunnel spin polarization (TSP), it may be desirable to use highly ordered tunnel contacts with MgO(001) tunnel barriers and bcc ferromagnets (FMs) [6, 14, 27]. Studies on the effect of such a highly ordered tunnel contact on the spin signals in Si are very demanding.

This paper shows that the spin signals in CoFe/MgO/n-Si, investigated by means of a three-terminal Hanle (TTH) method, are very much influenced by the properties of the tunnel contacts. In addition, an unconventional Hanle effect is observed in a highly ordered CoFe/MgO/Si system with bias and temperature variations. We find that (i) the spin signal and effective spin lifetime obtained in this system show non-monotonic bias and temperature dependence; (ii) the sign of the spin signal changes remarkably with the bias voltage at a low temperature.
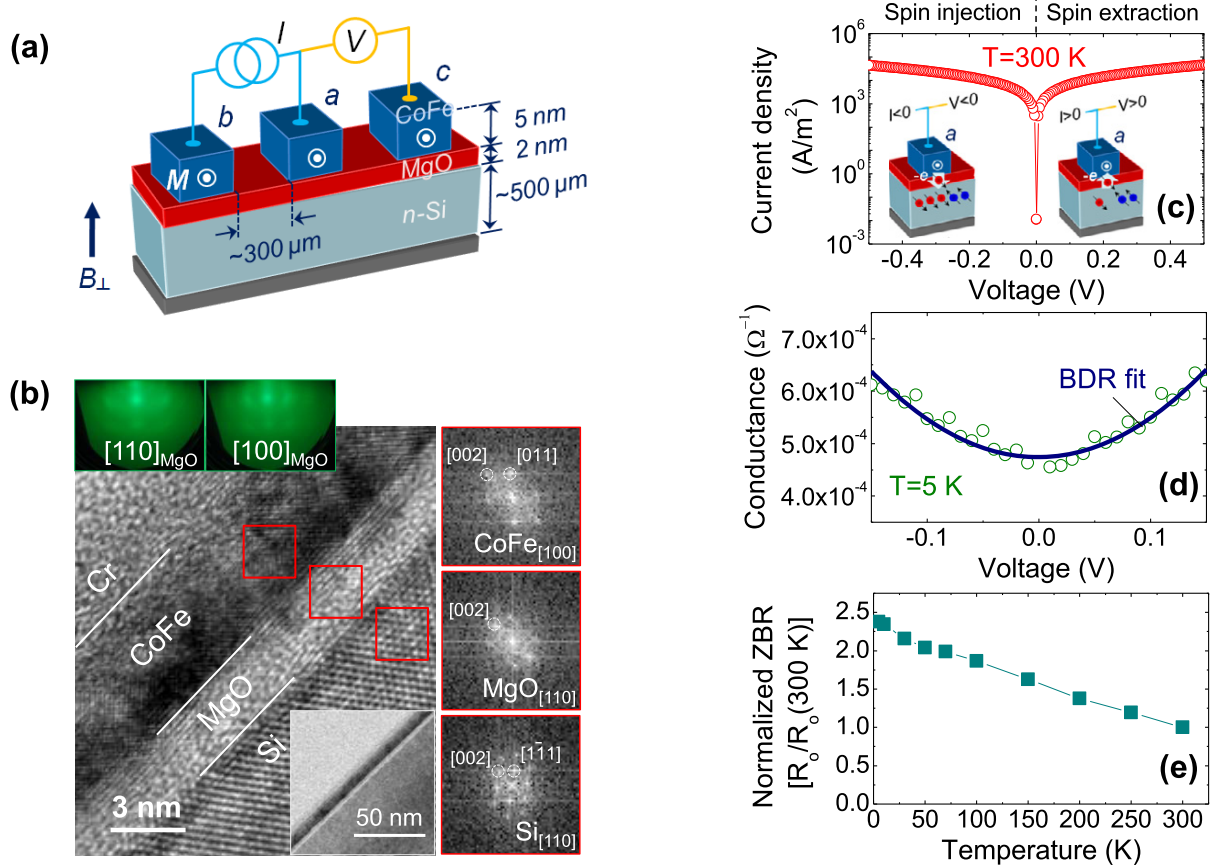
Figure 1. (a) Schematic diagram of the device geometry and TTH method. I_{ab} is the applied current flowing from contact a to contact b, and V_{ac} denotes the voltage measured between the contacts a and c. (b) High-resolution TEM image of the CoFe(5 nm)/MgO(2 nm)/Si sample. Left: low-magnification TEM image of the sample. The zone axis is parallel to the [110] direction of Si. Top: *in situ* RHEED patterns of the MgO along the azimuths of $Si_{[110]}$ and $Si_{[100]}$. Right: corresponding diffractograms for the regions (red rectangles) of the CoFe, MgO and Si in the sample. (c) Typical $J–V$ characteristics of the CoFe(5 nm)/MgO(2 nm)/n-Si tunnel contact at 300 K. (d) BDR fit (solid line) to the $G–V$ curve at 5 K. (e) Temperature dependence of ZBR (normalized).

2. Experimental details

Figure 1(a) shows a schematic diagram of the device geometry used in this study. We fabricated a symmetric device consisting of three highly ordered CoFe/MgO/n-Si tunnel contacts ($a–c$, $100 \times 150\,\mu m^2$). The contacts a (used as a spin injector/extractor and also as a spin detector) and b/c (used as references) are separated by about $300\,\mu m$ from each other, which is much longer than the spin diffusion length. The measurement scheme in figure 1(a), known as the TTH method [5, 16, 18, 19, 28, 29], provides a simple way to study the electrical spin injection and accumulation ($\Delta\mu = \mu^\uparrow - \mu^\downarrow$) in an SC. The TTH method has limitations for the reason that a quantitative analysis of the obtained spin signal is difficult compared to non-local Hanle

measurements and because it cannot fully uncover whether the measured spin accumulation comes from the bulk SC channel [19] or the localized states at the interface [18]. Nevertheless, the TTH enables us to investigate the effect of the tunnel-contact property on the spin signal with temperature (T) and bias voltage (V_0) variations.

The highly ordered CoFe(5 nm)/MgO(2 nm)/n-Si(001) (As-doped, $\rho \approx 2\, \text{m}\Omega\, \text{cm}$, $n_d \approx 2.5 \times 10^{19}\, \text{cm}^{-3}$) contacts were prepared by molecular beam epitaxy following a fabrication process described in the literature [30]. Figure 1(b) shows the *in situ* reflective high-energy electron diffraction (RHEED) patterns of the MgO(2 nm) layer, low-magnification and high-resolution transmission electron microscope (TEM) images, and diffractograms of the CoFe(5 nm)/MgO(2 nm)/n-Ge tunnel structure. The RHEED image of MgO grown on Si at 125 °C shows a spotty crystalline pattern, exhibiting a highly textured structure with an in-plane crystallographic relationship of MgO(001)[100]∥Si(001)[100]. The homogeneity of the CoFe/MgO and MgO/Si interfaces was checked by a low-magnification TEM image. The high-resolution TEM image and diffractograms confirm the highly (001) textured structure and the in-plane crystallographic relationship of CoFe(001)[110]∥MgO(001)[100]∥Si(001)[100], which is in agreement with a previous report [31].

Figure 1(c) shows the $J–V$ characteristics of the CoFe(5 nm)/MgO(2 nm)/n-Si contacts at 300 K. We adopt the convention that a negative applied current ($I < 0$) corresponds to electron spin injection ($V < 0$) and a positive applied current ($I > 0$) corresponds to electron spin extraction ($V < 0$) (see the insets of figure 1(c)). The figure exhibits nonlinear and quasi-symmetric behavior with respect to zero bias, indicating that the MgO tunnel barrier plays a dominant role in electronic transport. We obtained a reasonable fit (figure 1(d)) to the $G–V$ curve in the low bias region ($\pm 150\, \text{mV}$) using the Brinkman, Dynes and Rowell (BDR) model [32] with a barrier thickness of ~ 20 Å (determined from the TEM). The BDR fit gives the average barrier height of ~ 2.03 eV and its asymmetry of ~ 0.05 eV at 5 K. The T dependence of the normalized zero bias resistance (ZBR) in figure 1(e), defined as $R_0(T)/R_0(300\, \text{K})$, shows weak insulator-like behavior, indicating a pinhole-free tunnel barrier. These results confirm that the basic transport mechanism in this contact is tunneling.

3. Results and discussion

3.1. Electrical injection and detection of spin accumulation in a CoFe/MgO/Si contact at 300 K

At the beginning of each Hanle measurement, we applied a large enough in-plane magnetic field (>1 T) along the easy $[100]_{\text{CoFe}}$ axis (parallel to the long axis of the contacts in the device) to create homogeneous in-plane magnetization in each contact, after which the in-plane field was reduced to zero. To verify the magnetic homogeneity of the spin-tunnel contact, we investigated the magnetic domain structure of a Cr(2 nm)/CoFe(5 nm)/MgO(2 nm)/Si(001) reference sample using a magneto-optical microscope magnetometer (MOMM) [33, 34] and a vibrating sample magnetometer (VSM). A combined study using an MOMM and a VSM confirms that the CoFe layer in the contact has clear magnetic switching with almost uniform magnetization (not shown). In addition, the magnetic hysteresis curves are very well explained by the rotation of the uniform magnetization. The spin accumulation ($\Delta \mu$) in the CoFe/MgO/n-Si contact was measured by the voltage changes ($\Delta V_{ac} \propto \Delta \mu$) as a function of the perpendicular magnetic field ($B_\perp$) while keeping the constant current (I_{ab}). If we define V_0 by $V_0 = V_{ac}$ at $B_\perp = 0$ and V_{00} as
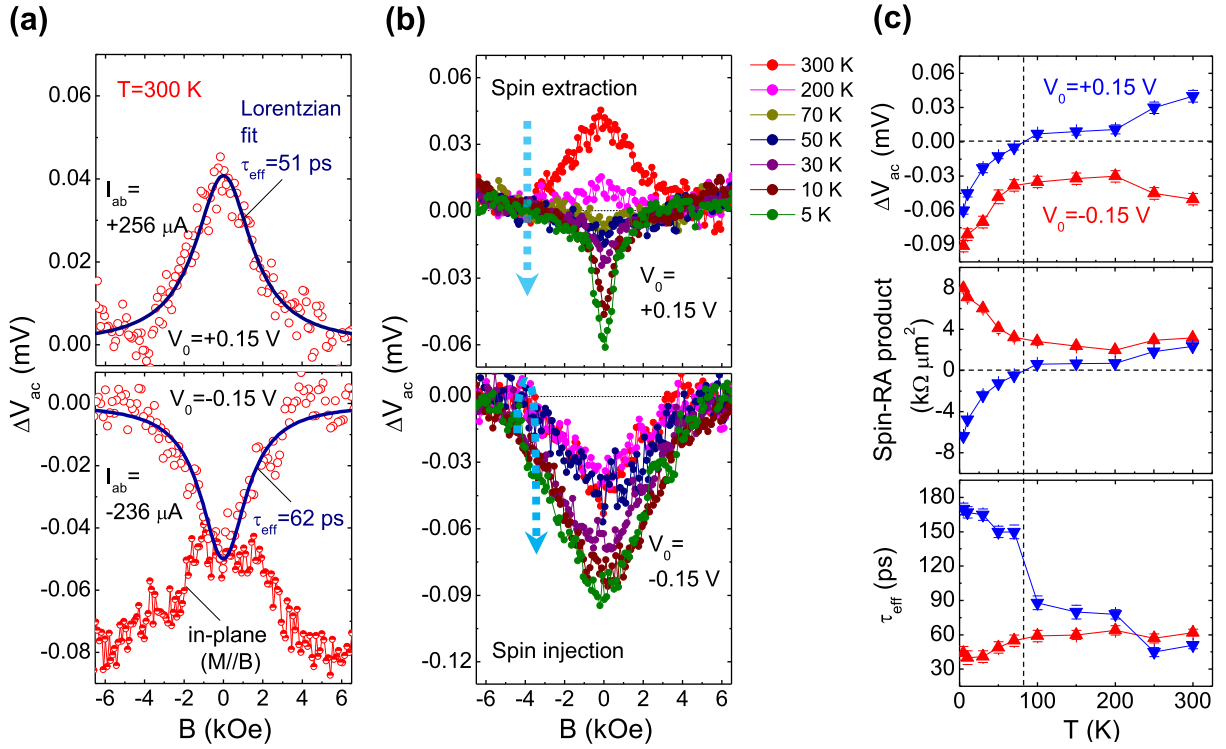
Figure 2. (a) Electrical Hanle signals (ΔV_{ac}) across the CoFe/MgO/n-Si tunnel contact as a function of the perpendicular magnetic field ($B_\perp$) at 300 K for applied currents (I_{ab}) of $-236/+256\,\mu$A ($\mp$, spin injection/extraction), corresponding to $V_{ac} = \mp 0.15$ V at $B_\perp = 0$ (or $V_0 = \mp 0.15$ V). The solid lines represent the Lorentzian fits. The half closed circle shows the in-plane measurement ($M \parallel B$). It should be noted that the bias voltage (V_0) is defined as V_{ac} at $B_\perp = 0$. (b) Electrical Hanle signals (ΔV_{ac}) versus the perpendicular magnetic field ($B_\perp$) over the temperature range of 5–300 K at bias voltages (V_0) of ∓ 0.15 V for the tunnel contact. The bias currents varied from $-171/+141\,\mu$A (5 K) to $-236/+256\,\mu$A (300 K). (c) Electrical Hanle signals (ΔV_{ac}), spin RA products ($\Delta V_{ac}/J_{ab}$), and effective spin lifetimes (τ_{eff}) versus the temperature (T) at bias voltages (V_0) of ∓ 0.15 V ($-/+$, spin injection/spin extraction).

the interpolated base line of V_{ac} with no spin accumulation, ΔV_{ac} can be determined as $V_0 - V_{00}$. As shown in the $\Delta V - B_\perp$ plots in figure 2(a), clear and large Hanle signals of $\Delta V_{ac,\mp} \approx (-)0.05/(+)0.04$ mV ($-/+$, spin injection/spin extraction) were obtained at 300 K with the applied currents (I_{ab}) of $-236/+256\,\mu$A ($V_{ac} = \mp 0.15$ V at $B_\perp = 0$, or $V_0 = \mp 0.15$ V). The corresponding spin resistance-area (RA) products ($\Delta V_{ac,\mp}/J_{ab}$) are 3.2/2.3 k$\Omega\,\mu$m^2, which are comparable to that of a Co/NiFe/AlO/n-Si contact [5]. The Hanle signals can be described fairly well by a Lorentzian function [28, 29, 35], $\Delta V_\mp(B_\perp) = \Delta V_\mp(0)/(1 + (\Omega\tau_{\text{sf},\mp})^2)$ with $\Omega = g\mu_B B_\perp/\hbar$. Here, g is the Landé g-factor, μ_B is the Bohr magneton and $\tau_{\text{sf},\mp}$ is the spin lifetime. Using a Lorentzian fit and taking an electron g-factor of 2 for the n-Si, we estimated effective spin lifetimes ($\tau_{\text{eff},\mp}$) of 62($-$)/51($+$) ps for heavily doped Si at 300 K. Such timescales are much smaller than the expected spin lifetime (of the order of ns) from the Elliott–Yafet spin

relaxation rate [36, 37]. We believe that the measured spin lifetime is a lower limit, and the true spin lifetime may be longer than $\tau_{\text{eff}, \mp} = 62(-)/51(+)$ ps. According to a recent report [38], the local magnetostatic fields due to the finite roughness of the FM/oxide interface strongly reduce the spin accumulation at the SC interface and artificially broaden the Hanle curve. As proven by the in-plane measurement ($M \parallel B$) of the inverted Hanle effect [38], shown at the bottom of figure 2(a), the interfacial spin depolarization effect is considered to be the main origin of the unexpectedly broadened Hanle curve in the CoFe/MgO/Si contact. Hence, the extracted values (from the Hanle curve with a Lorentzian fit) should be treated as the lower limit (or effective value) of the spin lifetime.

3.2. Non-monotonic temperature dependence of spin signal

One of the most important features in our data is the non-monotonic change of the Hanle curves with the T variation. Figure 2(b) shows the voltage changes (ΔV_{ac}) versus the perpendicular magnetic field ($B_\perp$) for the T range of 5–300 K when $V_0 = \mp 0.15$ V. Strikingly, the magnitude and width of the signal do not vary monotonically with T (cyan arrows) and the Hanle signal is, in fact, inverted at a low T in the spin extraction condition ($V_0 = +0.15$ V). It should be noted that this sign inversion is different from the inverted Hanle effect [38] in the in-plane measurement ($M \parallel B$), as this curve is measured with a perpendicular magnetic field. This behavior is clearly in contrast with that of the Co/NiFe/AlO/n-Si contact, where the measured Hanle curve changes monotonically as T decreases [5].

For a quantitative analysis, we plotted the electrical Hanle signal (ΔV_{ac}), the spin RA product (or spin signal, $\Delta V_{ac}/J_{ab}$) and the effective spin lifetime (τ_{eff}) as a function of T at V_0 values of ∓ 0.15 V ($-/+$, spin injection/spin extraction) in figure 2(c). The spin RA product (figure 2(c)) is useful in characterizing the obtained Hanle signal. At -0.15 V, the spin RA product remains almost constant as T is decreased to 100 K. It gradually increases as T is decreased further to 5 K, showing no sign inversion. In contrast, the spin signal measured at $+0.15$ V initially decreases ($T > 100$ K), crosses zero and finally increases in the negative direction below 70 K. The sign change of the signal from positive ($T > 100$ K) to negative ($T < 70$ K) will be discussed in the following sections.

As shown in the bottom panel of figure 2(c), the τ_{eff} value at $+0.15$ V continually increases from 51 ps at 300 K to 170 ps at 5 K. In contrast, at -0.15 V, a weak variation of τ_{eff} with T is observed, implying unequal momentum scattering rates [36, 37] for the injected and extracted electrons.

3.3. Single-step tunneling model

Given the symmetric J–V curves with weak T dependence (figures 1(c) and (e)) and the small RA values of the contact ($\sim 1 \times 10^{-5}$ Ωm^2 (300 K) to $\sim 2 \times 10^{-5}$ Ωm^2 (5 K) at -0.15 V), we analyzed the observed spin signals based on the single-step tunneling [3, 18] using the following expressions:

$$\frac{\Delta V}{J} = \frac{\gamma_d \Delta\mu/(-2e)}{J}, \quad \Delta\mu \approx (-2e)\gamma_{i/e} J \, r_{\text{ch}} = (-2e)\gamma_{i/e} J \rho \, l_{\text{sf}}.$$

Here, γ_d is the TSP value corresponding to the detection of the induced spin accumulation at the Si interface, $\gamma_{i/e}$ is the TSP of the injected/extracted electrons, r_{ch} is the spin-flip resistance associated with the Si channel, ρ is the resistivity of Si and l_{sf} is the spin diffusion length in Si.
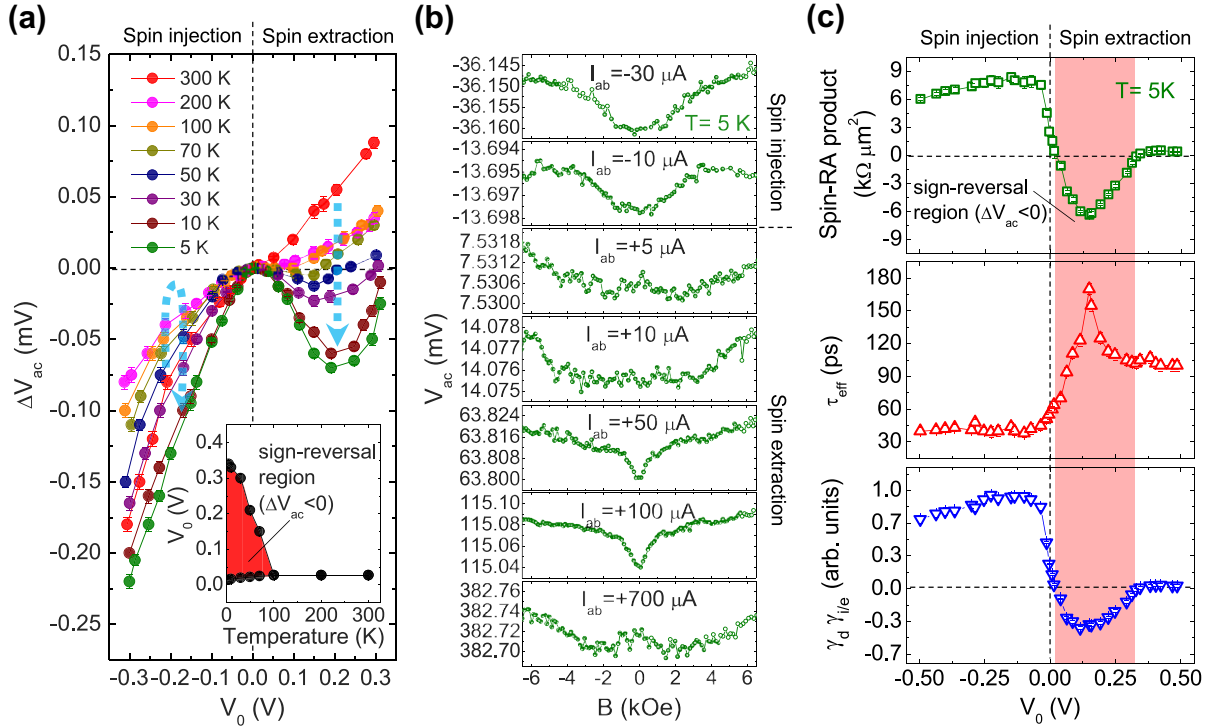
Figure 3. (a) Electrical Hanle signal (ΔV_{ac}) versus the bias voltage (V_0) up to ± 0.3 V over the entire temperature range of 5–300 K. The applied current (I_{ab}) range varied from $+0.40/-0.45$ mA (5 K) to $+1.00/-0.75$ mA (300 K). The inset shows the sign-reversal region ($\Delta V_{ac} < 0$, under a forward bias) during the variation of temperature. (b) Hanle curves obtained at 5 K for both bias polarities. (c) Associated spin signal ($\Delta V_{ac}/J_{ab}$) and effective spin lifetime (τ_{eff}) in the bias range of ± 0.5 V ($+1.35/-1.10$ mA) at 5 K. The V_0 dependence of $\gamma_{\text{d}} \gamma_{\text{i/e}}$ (normalized) was deduced from equation (1) using the $\Delta V_{ac}/J_{ab}$ and τ_{eff} values.

In the degenerate regime of an SC [3], the value of l_{sf} is given by $\sqrt{\tau_{\text{sf}}/4e^2N(E_{\text{F}})\rho}$, where $N(E_{\text{F}})$ is the density of states (DOS) for Si. Because the ρ and $N(E_{\text{F}})$ values of heavily doped Si show weak T dependence [5], the spin signal should vary with T, as $\Delta V/J \propto \gamma_{\text{d}}\gamma_{\text{i/e}}\sqrt{\tau_{\text{sf}}}$. Therefore, the increase of $\Delta V_{ac}/J_{ab}$ at a low T is a direct consequence of the corresponding enhancement [14] of $\gamma_{\text{d}} \gamma_{\text{i/e}}$ (figure 2(c)). The sign inversion of $\Delta V_{ac}/J_{ab}$ at a low T for spin extraction ($V_0 = +0.15$ V) is also closely related to the sign change of $\gamma_{\text{d}} \gamma_{\text{e}}$.

3.4. Sign inversion of the spin signal with a bias voltage at low temperature

Another noteworthy finding is that the sign of the spin signal also changes with V_0 in the TTH measurements. Figure 3(a) shows the ΔV_{ac} versus V_0 plot over the entire temperature range of 5–300 K (note that we utilized the ΔV_{ac} versus V_0 plot instead of the ΔV_{ac} versus I_{ab} plot to specifically analyze the bias dependence with energy dimensions). When $T > 100$ K, ΔV_{ac} increases with V_0, showing negligible asymmetry with respect to the bias polarity. However, when $T < 100$ K, a peculiar bias dependence with significant asymmetry arises. Interestingly, a negative value of ΔV_{ac} is observed in a low forward bias range ($+25$ mV $< V_0 < +150$ mV)

at 70 K. When T is decreased further, the region showing a negative sign gradually expands toward a higher bias, as shown in the inset of figure 3(a).

Figure 3(b) shows the Hanle curves obtained at 5 K for both bias polarities. The $\Delta V_{ac,-}$ in the negative bias range, corresponding to the electron injection from CoFe to Si, is negative, as shown in the top two curves obtained at -36.2 and -13.7 mV ($I_{ab} = -30\,\mu A$, and $I_{ab} = -10\,\mu A$, respectively). Additionally, $\Delta V_{ac,+}$ at a small forward bias at $+7.5$ mV ($I_{ab} = +5\,\mu A$) is positive, as expected from the conventional Hanle effect. However, when the forward bias is increased, $\Delta V_{ac,+}$ almost disappears at $+14.1$ mV ($I_{ab} = +10\,\mu A$), becoming negative in a larger forward bias range. With further increase in the bias ($V_0 > +340$ mV or $I_{ab} > +700\,\mu A$), the sign of $\Delta V_{ac,+}$ is switched again and eventually becomes positive. The associated values of $\Delta V_{ac}/J_{ab}$ and τ_{eff} are summarized in figure 3(c) up to ± 0.5 V.

The peculiar bias dependence of the spin RA product ($\Delta V/J$) can be understood in terms of the bias dependence of $\gamma_d \gamma_{i/e}$. As discussed in section 3.3, $\Delta V/J$ is proportional to $\gamma_d \gamma_{i/e} \sqrt{\tau_{sf}}$ at a given T, and $\gamma_d \gamma_{i/e}$ strongly influences the value of $\Delta V/J$. Using $\Delta V_{ac}/J_{ab}$ and τ_{eff} values, we estimated the V_0 dependence of $\gamma_d \gamma_{i/e}$ (normalized), as shown in figure 3(c). In the reverse bias region ($V_0 < 0$, spin injection), the magnitude of $\gamma_d \gamma_i$ is relatively large with weak V_0 dependence. In contrast, in the forward bias region, the $\gamma_d \gamma_e$ value shows peculiar bias dependence, including an inversion of its sign.

Sign inversion of the spin signal was previously observed in non-local spin valve measurements with semiconducting spin channels [10, 24, 25, 39]. The inversion of the Hanle signal for the relative magnetic configuration [10, 14] (parallel or anti-parallel) in non-local Hanle measurements originates from the change of sign in $\gamma_d \gamma_{i/e}$. It should be mentioned that the Hanle effect always reduces the absolute value of spin accumulation ($|\Delta \mu|$), but the polarity [10, 11, 14] of the Hanle curve is determined by the sign of $\gamma_d \gamma_{i/e}$. Note that

$$\Delta V = \frac{\gamma_d \left|\gamma_{i/e}\right| |\Delta\mu|}{(-2e)\gamma_{i/e}}.$$

For $\gamma_d \gamma_{i/e} > 0$, a normal Hanle curve is observed; on the other hand, for $\gamma_d \gamma_{i/e} < 0$, an inverted Hanle curve is obtained. Although the same contact is used for both spin injection and spin detection in the TTH measurements, the sign of γ_d is not necessarily the same as the sign of $\gamma_{i/e}$.

Even in metallic tunnel junctions, it is possible for the TSP of the tunnel contact to have either positive or negative values depending on the bias voltage; the very same tunnel barrier can have positive TSP at one bias and negative TSP at other biases. There are numerous examples of these phenomena in magnetic tunnel junctions (MTJs). For instance, Moodera *et al* [40] reported the asymmetric bias dependence and sign inversion of the tunnel magnetoresistance (TMR) in $Co/Au/Al_2O_3/NiFe$ MTJs with quantum well states in the structure. De Teresa *et al* [41] showed that the sign of the TMR is reversed in a small bias range in epitaxial $Co/SrTiO_3/La_{0.7}Sr_{0.3}MnO_3$ MTJs and that the metal/oxide interface plays an important role in determining the spin polarization of electrons tunneling from or into ferromagnetic transition metals. LeClair *et al* [42] showed that the asymmetry and inversion of TMR occur due to the band structure and DOS effects in Co-based MTJs. Greullet *et al* [43] reported a large inverse TMR in fully epitaxial $Fe/Fe_3O_4/MgO/Co$ MTJs, which is strongly dependent on the bias voltage.

In the same vein, the observed sign change in the CoFe/MgO/Si contact appears to be closely associated with the asymmetrical bias dependence of tunneling phenomena. The injected electrons from the FM metal to SC have a narrow energy distribution near the Fermi level (E_F)

in CoFe [44], whereas the energy level of electrons extracted from the SC to FM metals can be strongly dependent on the electron states in SC.

3.5. Spin extraction process via the interfacial resonant state at CoFe/MgO or bound states in Si

The sign inversion of $\gamma_d \gamma_e$ at a finite forward bias ($V_0 > 0$, spin extraction) in figure 3(c) can be understood in terms of the spin extraction process through the interfacial resonant states (IRSs) [20, 21, 26] formed at the CoFe/MgO interface or the bound states (BSs) [22] in the Si surface, as depicted in figures 4(a) and (b). Three mechanisms for the inversion of the spin polarization in FM/SC Schottky contacts have been proposed: (i) transmission probability [21, 23] depending on the Schottky barrier profile of the SC, (ii) resonant tunneling via IRSs [20, 21, 26] at the FM/SC interface and (iii) tunneling from BSs [22, 45] in a heavily doped layer near the SC surface. As the electronic transport of our contact is dominated by the MgO tunnel barrier and not by the Schottky barrier (see figures 1(c)–(e)), the latter two mechanisms are more probable in our system: (ii) the interfacial bonding effect of CoFe–Mg may change the CoFe surface states [20, 46], which may cause the IRSs to favor the extraction of minority-spin electrons and (iii) the inhomogeneous doping accumulation at the Si surface during the annealing process (e.g. pre-annealing at 500 °C, post-annealing at 300 °C) may create BSs from which preferentially extracted spins are in the minority [22].

3.6. Weighting of majority-spin and minority-spin extraction processes and associated Hanle effects

Figure 4 shows a schematic illustration of the possible spin extraction processes from Si to CoFe and the associated Hanle effects. We limit our picture for the case of a positive γ_d value, as it is not possible to unambiguously determine each sign of TSPs (γ_d, γ_e) by means of TTH measurements. Thus, the CoFe prefers to align its E_F with the electrochemical potential ($\mu_\uparrow$) of the majority-spin in Si (see black circles and arrows in figures 4(c) and (f)).

The sign and magnitude of the accumulated spin in Si (under forward bias) are determined by the weighting of the majority-spin and minority-spin extraction processes [24]. The direct tunneling through a highly ordered MgO(001) barrier strongly favors majority-spin extraction owing to the symmetry conservation and spin filtering of *bulk* CoFe and Si wave functions [27]. On the other hand, the IRSs [20, 21, 26] formed at the CoFe/MgO interface or BSs [22, 45] in the Si surface promote minority-spin extraction. Because the contribution of the IRSs and BSs has a finite energy window, the applied forward bias can modify the contribution of those states to the total amount of tunneling conductance.

It is believed that the peaks around $V_0 \approx +150$ mV in the sign-reversal regime (figures 3(a) and (c)) are associated with the dominant contribution of the minority-spin extraction processes. At a forward bias voltage of $V_0 \approx +150$ mV, IRSs formed at the CoFe/MgO interface (figure 4(a)) or the BSs in the Si surface (figure 4(b)) promote minority-spin extraction ($\gamma_e < 0$), resulting in majority-spin accumulation ($\Delta\mu > 0$) in the Si. In this case, an inverted Hanle curve is observed (because $\gamma_e \gamma_d < 0$); the minimum voltage signal is obtained at $B_\perp = 0$, and it gradually increases as $B_\perp$ increases (see figure 4(c)). The τ_{eff} versus V_0 plot (figure 3(c)) also shows a peak at $V_0 \approx +150$ mV, which coincides with the bias range where the sign inversion of the Hanle curve and the negative $\gamma_d \gamma_e$ value are observed. The enhancement of τ_{eff} is presumably
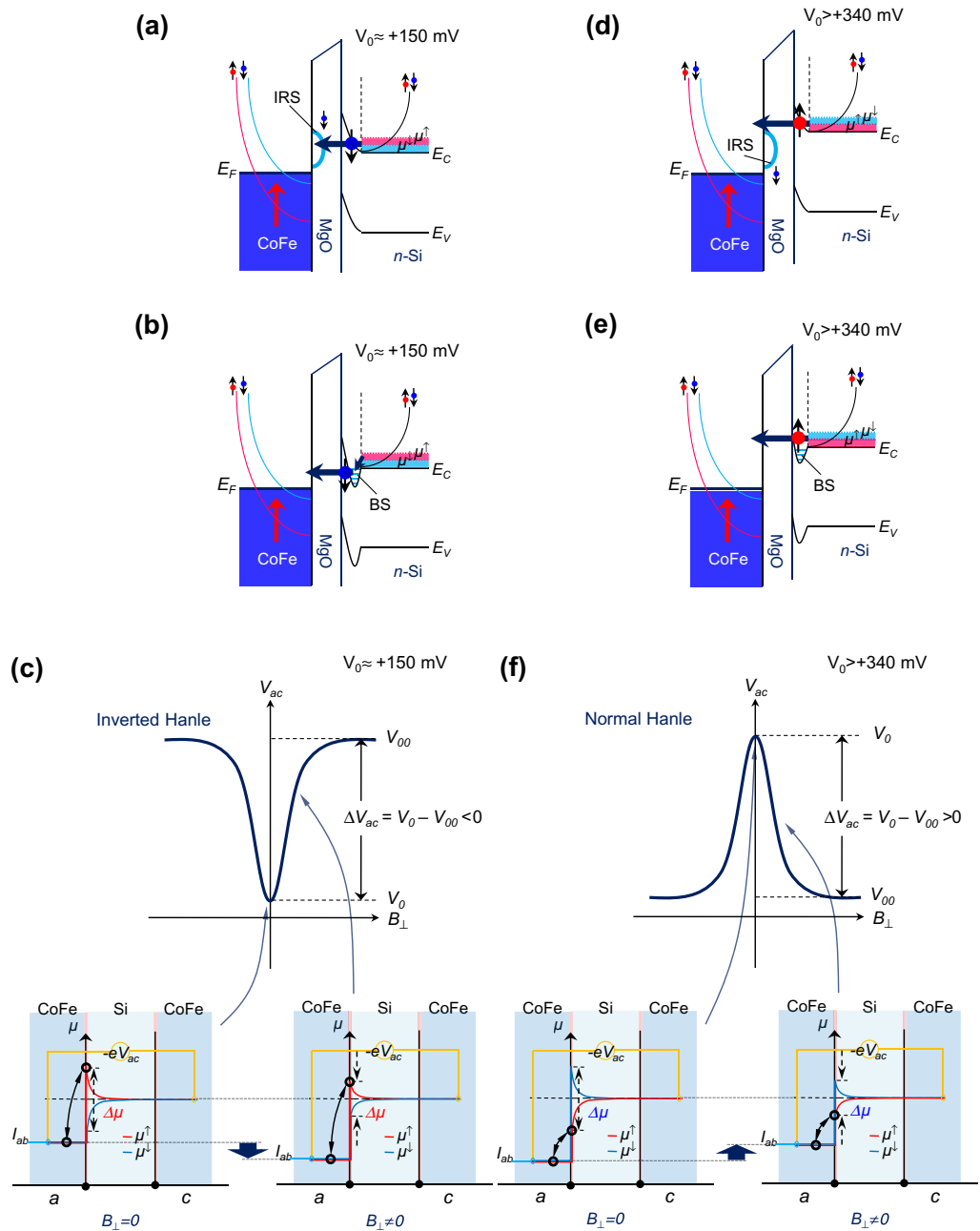
Figure 4. Possible spin extraction processes from Si to CoFe through the IRSs formed at the CoFe/MgO interface ((a) and (b)) or BSs in the Si surface ((d) and (e)) at two different forward bias regimes as indicated in the figures ($V_0 \approx +150\,\text{mV}$ and $V_0 > +340\,\text{mV}$). Parabolic dispersion $E(k)$, representing the simplified majority (red)/minority (blue) spin bands of an FM, is depicted in the energy band diagram. (c) and (f) Associated Hanle curves and the illustrations of spin accumulation in Si, where the red and blue lines represent, respectively, the spin-up ($\mu_\uparrow$, majority-spin) and spin-down ($\mu_\downarrow$, minority-spin) electrochemical potentials. Note that we limit our picture to the case of a positive γ_d value, as it is not possible to unambiguously determine each sign of TSPs (γ_d, γ_e) by means of TTH measurements.

related to the tunneling process via the IRSs at the CoFe/MgO interface or the BSs in the Si surface, implying that the spin flip scattering is restricted in these states.

At a high forward bias ($V_0 > +340$ mV), majority-spin is preferentially extracted from Si to CoFe ($\gamma_e > 0$, see figures 4(c) and (d)) owing to the direct tunneling through the highly ordered MgO (001) [22, 27], resulting in minority-spin accumulation ($\Delta\mu < 0$) in Si. Thus, a normal Hanle curve is observed (because $\gamma_e \gamma_d > 0$); the maximum voltage signal is obtained at $B_\perp = 0$, and it gradually decreases with an increase in $B_\perp$ (see figure 4(f)).

4. Conclusions

In conclusion, we experimentally observed an unconventional Hanle effect in a highly ordered CoFe/MgO/n-Si system using the TTH method. We find that the spin signal and effective spin lifetime of the CoFe/MgO/n-Si contact show non-monotonic behavior with bias and temperature variations. Furthermore, sign inversion of the spin signal was observed at a low temperature, which is likely related to the spin extraction process via IRSs at the CoFe/MgO or BSs in the Si.

Acknowledgments

Appendix

An important insight can be obtained from the high-field TTH measurements (up to ± 3 T) on the CoFe/MgO/Si contact under a perpendicular ($M \perp B$, red) and an in-plane ($M \parallel B$, blue) magnetic field. As shown in figures A.1(a)–(d), three distinct regions were observed in the $M \perp B$ measurement (red): (i) the Hanle effect at small magnetic fields, (ii) the rotation of the magnetization (M) and (iii) the saturation of M. As $B_\perp$ is increased, the voltage signal from the spin accumulation is sharply reduced/increased (by the sign of $\gamma_d \gamma_{i/e}$) due to the Hanle effect in region (i), after which it gradually increases when the M of the FM rotates out of the plane in region (ii). When the M and induced spin accumulation in the SC are fully aligned with $B_\perp$ higher than the demagnetization field (~ 2.2 T) of CoFe, the voltage signal eventually becomes saturated in region (iii). On the other hand, the $M \parallel B$ measurement (figures A.1(a)–(d), blue) reveals moderate behavior, showing an inverted Hanle effect [38]. At zero or small external magnetic field, the injected spins are precessed and dephased by local magnetostatic fields having random directions, resulting in a reduction of the spin accumulation. In contrast, a larger external magnetic field ($B_\parallel$) can eliminate the local magnetostatic fields, restoring full spin accumulation. In figures A.1(a)–(c), one can see that the difference in the voltage signals ($V_{ac}(B_\perp)$, $V_{ac}(B_\parallel)$) in the saturation region (iii), which may be due to the tunneling anisotropic magnetoresistance [47]. The overall behavior of the voltage signals (for the perpendicular and in-plane fields) is in good agreement with that of the FM/Al$_2$O$_3$/Si and Co/Al$_2$O$_3$/GaAs contacts [38].
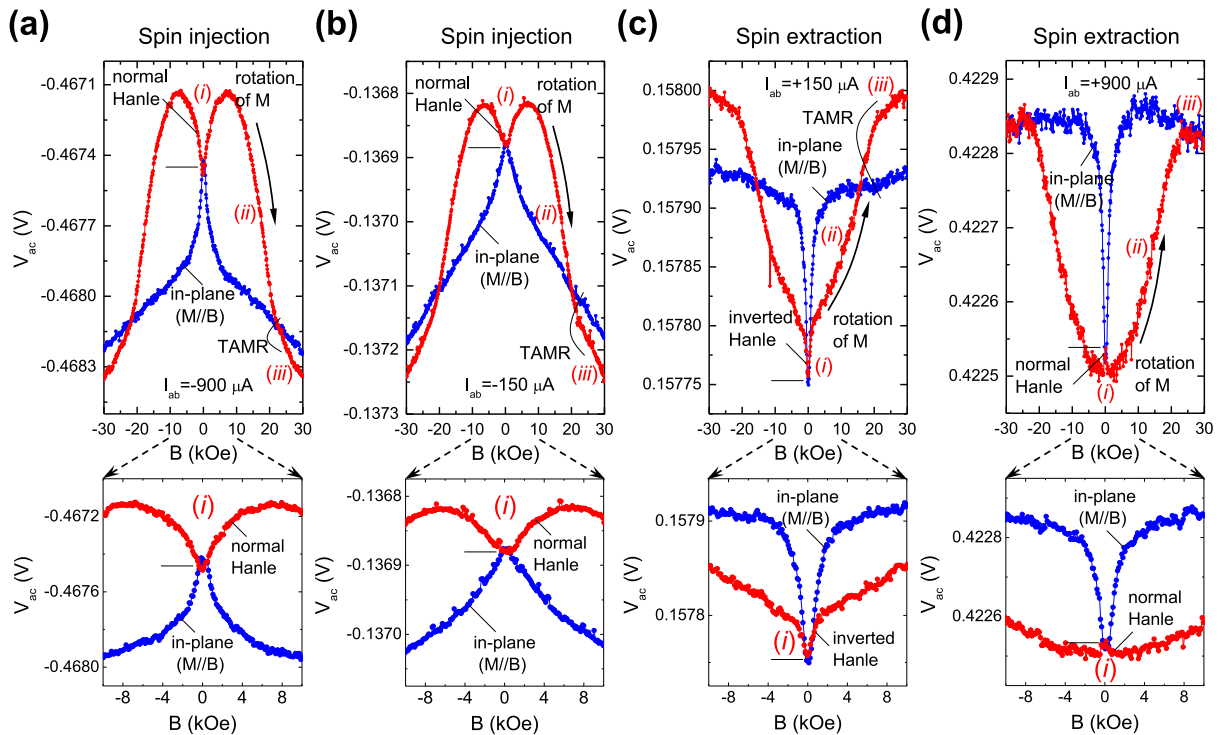
Figure A.1. High-field Hanle measurements for the CoFe/MgO/*n*-Si contact at 5 K. (a)–(d) *B* (up to ±3.0 T) is applied perpendicular to the interface plane (red) or parallel to the interface (blue). The bottom panels show expanded views of the low-field range (up to ±1.0 T).

References

[1] Wolf S A, Awschalom D D, Buhrman R A, Daughton J M, von Molnár S, Roukes M L, Chtchelkanova A Y and Treger D M 2001 *Science* **294** 1488

[2] Zutić I, Fabian J and Das Sarma S 2004 *Rev. Mod. Phys.* **76** 323

[3] Fert A and Jaffrès H 2001 *Phys. Rev.* B **64** 184420

[4] Min B C, Motohashi K, Lodder J C and Jansen R 2006 *Nat. Mater.* **5** 817

[5] Dash S P, Sharma S, Patel R S, de Jong M P and Jansen R 2009 *Nature* **462** 491

[6] Jiang X, Wang R, Shelby R M, Macfarlane R M, Bank S R, Harris J S and Parkin S S P 2005 *Phys. Rev. Lett.* **94** 056601

[7] Hanbicki A T, Jonker B T, Itskos G, Kioseoglou G and Petrou A 2002 *Appl. Phys. Lett.* **80** 1240

[8] Motsnyi V F, De Boeck J, Das J, Van Roy W, Borghs G, Goovaerts E and Safarov V I 2002 *Appl. Phys. Lett.* **81** 265

[9] Jonker B T, Kioseoglou G, Hanbicki A T, Li C H and Thompson P E 2007 *Nat. Phys.* **3** 542

[10] Lou X *et al* 2007 *Nat. Phys.* **3** 197

[11] Appelbaum I, Huang B and Monsma D J 2007 *Nature* **447** 295

[12] van 't Erve O M J, Hanbicki A T, Holub M, Li C H, Awo-Affouda C, Thompson P E and Jonker B T 2007 *Appl. Phys. Lett.* **91** 212109

[13] Ando Y, Hamaya K, Kasahara K, Kishi Y, Ueda K, Sawano K, Sadoh T and Miyao M 2009 *Appl. Phys. Lett.* **94** 182105

[14] Sasaki T, Oikawa T, Suzuki T, Shiraishi M, Suzuki Y and Noguchi K 2010 *Appl. Phys. Lett.* **96** 122101

[15] Ciorga M, Einwanger A, Wurstbauer U, Schuh D, Wegscheider W and Weiss D 2009 *Phys. Rev.* B **79** 165321

[16] Lou X, Adelmann C, Furis M, Crooker S A, Palmstrøm C J and Crowell P A 2006 *Phys. Rev. Lett.* **96** 176603

[17] Koo H C, Kwon J H, Eom J H, Chang J Y, Han S H and Johnson M 2009 *Science* **325** 1515

[18] Tran M, Jaffrès H, Deranlot C, George J-M, Fert A, Miard A and Lemaître A 2009 *Phys. Rev. Lett.* **102** 036601

[19] Jansen R, Min B C, Dash S P, Sharma S, Kioseoglou G, Hanbicki A T, van 't Erve O M J, Thompson P E and Jonker B T 2010 *Phys. Rev.* B **82** 241305

[20] Chantis A N, Belashchenko K D, Smith D L, Tsymbal E Y, van Schilfgaarde M and Albers R C 2007 *Phys. Rev. Lett.* **99** 196603

[21] Honda S, Itoh H, Inoue J, Kurebayashi H, Trypiniotis T, Barnes C H W, Hirohata A and Bland J A C 2008 *Phys. Rev.* B **78** 245316

[22] Dery H and Sham L J 2007 *Phys. Rev. Lett.* **98** 046602

[23] Smith D L and Ruden P P 2008 *Phys. Rev.* B **78** 125202

[24] Salis G, Fuhrer A, Schlittler R R, Gross L and Alvarado S F 2010 *Phys. Rev.* B **81** 205323

[25] Salis G, Alvarado S F and Fuhrer A 2011 *Phys. Rev.* B **84** 041307

[26] Wada E, Shirahata Y, Naito T, Itoh M, Yamaguchi M and Taniyama T 2010 *Phys. Rev. Lett.* **105** 156601

[27] Bulter W H, Zhang X G, Schulthess T C and MacLaren J M 2001 *Phys. Rev.* B **63** 054416

[28] Johnson M and Silsbee R H 1985 *Phys. Rev. Lett.* **55** 1790

[29] Johnson M and Silsbee R H 1988 *Phys. Rev.* B **37** 5326

[30] Jeon K R, Park C Y and Shin S C 2010 *Cryst. Growth Des.* **10** 1346

[31] Miao G X, Chang J Y, van Veenhuizen M J, Thiel K, Seibt M, Eilers G, Münzenberg M and Moodera J S 2008 *Appl. Phys. Lett.* **93** 142511

[32] Brinkman W F, Dynes R C and Rowell J M 1970 *J. Appl. Phys.* **41** 1915

[33] Choe S B, Kim D H, Cho Y C, Jang H J, Ryu K S, Lee H S and Shin S C 2002 *Rev. Sci. Instrum.* **73** 2910

[34] Kim D H, Choe S B and Shin S C 2003 *Phys. Rev. Lett.* **90** 087203

[35] Motsnyi V F, Van Dorpe P, Van Roy W, Goovaerts E, Safarov V I, Borghs G and De Boeck J 2003 *Phys. Rev.* B **68** 245319

[36] Elliott R J 1954 *Phys. Rev.* **96** 266
     Yafet Y 1963 *Solid State Physics* ed F Seitz and D Turnbull vol 14 (Academic: New York) p 1

[37] Cheng J L, Wu M W and Fabian J 2010 *Phys. Rev. Lett.* **104** 016601

[38] Dash S P, Sharma S, Le Breton J C, Peiro J, Jaffrès H, George J-M, Lemaitre A and Jansen R 2011 *Phys. Rev.* B **84** 054410

[39] Crooker S A, Garlid E S, Chantis A N, Smith D L, Reddy K S M, Hu Q O, Kondo T, Palmstrøm C J and Crowell P A 2009 *Phys. Rev.* B **80** 041305

[40] Moodera J S, Nowak J, Kinder L R and Tedrow P M 1999 *Phys. Rev. Lett.* **83** 3029

[41] De Teresa J M, Barthélémy A, Fert A, Contour J P, Montaigne F and Seneor P 1999 *Science* **286** 507

[42] LeClair P, Kohlhepp J T, van de Vin C H, Wieldraaijer H, Swagten H J M, de Jonge W J M, Davis A H, MacLaren J M, Moodera J S and Jansen R 2002 *Phys. Rev. Lett.* **88** 107201

[43] Greullet F, Snoeck E, Tiusan C, Hehn M, Lacour D, Lenoble O, Magen C and Calmels L 2008 *Appl. Phys. Lett.* **92** 053508

[44] Valenzuela S O, Monsma D J, Marcus C M, Narayanamurti V and Tinkham M 2005 *Phys. Rev. Lett.* **94** 196601

[45] Hu Q O, Garlid E S, Crowell P A and Palmstrøm C J 2011 *Phys. Rev.* B **84** 085306

[46] Li Y, Chye Y, Chiang Y F, Pi K, Wang W H, Stephens J M, Mack S, Awschalom D D and Kawakami R K 2008 *Phys. Rev. Lett.* **100** 237205

[47] Gould C, Ruster C, Jungwirth T, Girgis E, Schott G M, Giraud R, Brunner K, Schmidt G and Molenkamp L W 2004 *Phys. Rev. Lett.* **93** 117203